The Spacecraft Power Supply System

By D. C. BOMBERGER, D. FELDMAN, D. E. TRUCKSESS, S. J. BROLIN, and P. W. USSERY

(Manuscript received February 11, 1963)

The power supply system in the Telstar spacecraft consists of a solar cell plant to convert solar radiation to electrical energy when the satellite is illuminated by the sun, a 19-cell nickel-cadmium battery to store energy, and a regulation circuit to supply constant output voltages over a wide variation in input voltages. Additionally, the power supply system provides switching to conserve power and allow battery recharging during periods between communications experiments.

I. INTRODUCTION

The power supply system used in the Telstar spacecraft employs a solar cell plant which converts solar radiation to electrical energy when the satellite is illuminated by the sun. During periods of eclipse and/or peak power drain of transmission, reserve power is provided by a 19-cell, nickel-cadmium battery. To conserve power and allow battery recharging, continuous power is supplied only to those circuits in the satellite necessary for ground tracking and command. All others are turned off when not required.

1.1 *Characterization of Loads*

The electrical systems in the spacecraft are divided into three major parts:

(a) the communications repeater, which contains the microwave transmitter, microwave receiver and microwave beacon;

(b) the radiation damage and particle distribution experiment;

(c) the command receivers, telemetry system, and VHF beacon transmitter.

The microwave transmitter contains a traveling-wave tube, the only electron tube in the satellite. The power requirements for the traveling-wave tube total 15.8 watts.

A transistorized dc-to-dc high-voltage converter was designed to achieve the desired voltages. The single converter provides all the required TWT power. All subsystems employ solid-state devices as active circuit elements and operate at 16 volts.

The power requirements for the microwave receiver and beacon total 3.2 watts. Together with the microwave transmitter, the power requirements for the communications experiment amount to 19.0 watts.

The instrumentation for the radiation damage and particle distribution experiment requires approximately 0.3 watt. For reliability, two command receivers are employed, each requiring 1.0 watt; the 136-mc VHF beacon transmitter requires 1.8 watts. The VHF beacon transmitter and the command receivers are continuously powered and require a total of 3.8 watts. The telemetry system requires approximately 0.9 watt.

The programming of the systems by ground command results in a power drain profile having three major levels. The first is the continuous drain of the VHF beacon transmitter and command system. This totals 3.8 watts. A second level adds the telemetry and radiation experiments which may be commanded "on"; the second level brings the total to 5.0 watts. The third level adds the power requirements of the communication repeater, resulting in a maximum power demand of 24 watts distributed among the several subsystems. An experiment considered typical for any 24-hour period is shown in the power profile of Fig. 1. The power level shown includes the losses of the high-voltage converter for the TWT and of the main 16-volt regulator. The details of these circuits are covered in later sections of this paper.

1.2 *Power System Design Considerations*

In addition to the specific power requirements of the electronic loads described in the preceding section, there are several general requirements which must be met by the power system.

(*i*) *Temperature Range* — An objective of the spacecraft thermal design was to attain an electronic canister temperature as close to 70°F as possible, regardless of the satellite spin-axis orientation with regard to the sun, during full sunlight, during maximum eclipse and with an estimated decrease in solar plant power from an initial 14 watts to 7 watts after a two-year life. Normal temperature range for these conditions over a two-year period was calculated to be 32°F to 70°F. Operational design limits of 15°F to 90°F were established for compo-

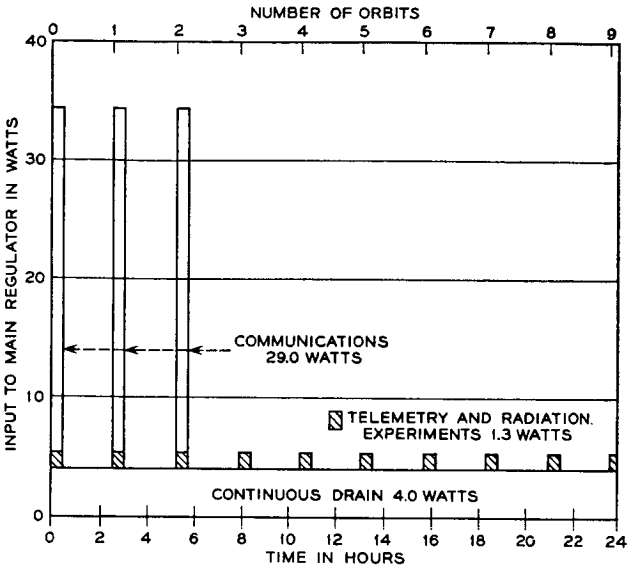

Fig. 1 — Power duty cycle referred to the input of the main regulator.

nents of the power system, and qualification tests include temperature checks at 0°F and 140°F.

(*ii*) *Efficiency and Weight* — Every effort was made to minimize the weight of the Telstar power system consistent with maintaining high power conversion efficiency, high reliability, and repeated operation in the radiation environment of the Van Allen belt. The battery and mounting weigh 11 pounds; the regulator and converter combined, including auxiliary control apparatus and wiring, weigh 7 pounds.

(*iii*) *Telemetry* — There are 30 channels of telemetry associated with the power system to provide information on its behavior. Battery voltage and temperature are monitored. The performance of the main regulator is assessed by monitoring various voltages and transistor case temperatures. The dc-to-dc converter is monitored by telemetering the heater voltage and collector current along with the helix and accelerator currents; in addition, the case temperature of switching transistors is monitored. Three channels are used to monitor the status of the relays associated with control sequence for commanding the TWT on. In addition, the current available from the solar cell plant is telemetered; this information, together with voltage measurements for the entire

nickel-cadmium storage battery, permits calculations of the available solar power to be readily made.

II. DESCRIPTION OF POWER SYSTEM

The Telstar power system employs silicon solar cells as the primary power source and a sealed nickel-cadmium storage battery which provides power for peak loads and for eclipse periods. An over-all block diagram is shown in Fig. 2. The number and arrangement of solar cells were designed to provide nearly constant power regardless of satellite attitude, at the value required to provide for the average power requirements of an orbit, including battery losses. The solar cell portion of the power system was designed to provide an initial power output of approximately 14 watts, which is sufficient to permit a flexible experimental program.

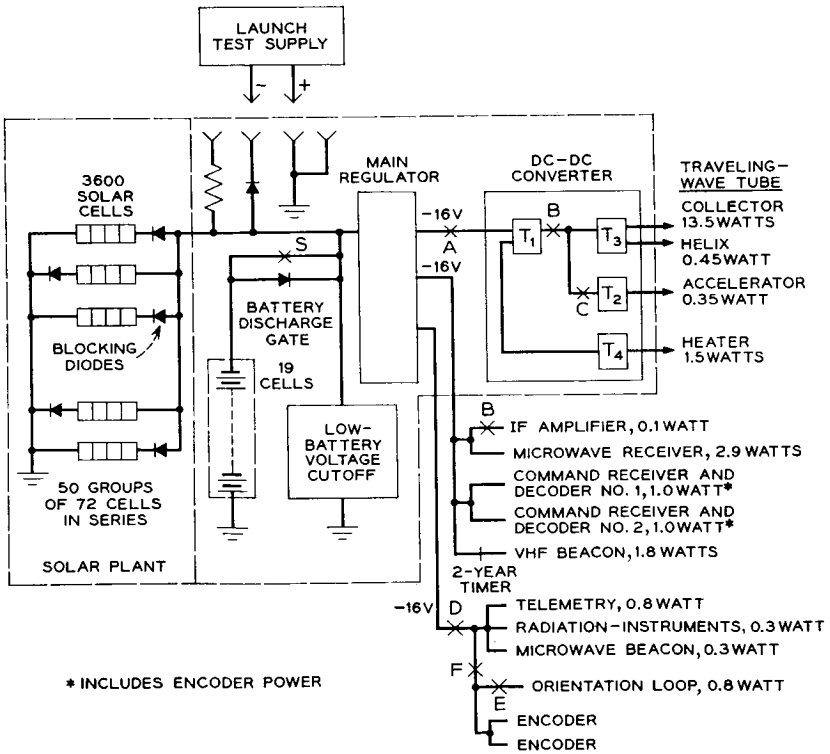

Fig. 2 — Block diagram of spacecraft power system.

The early objectives for the spacecraft included a minimum capability of 30 minutes per orbit for monitoring the telemetry and radiation experiments, with continuous use representing a desirable upper limit. An objective of at least 90 minutes per day was established for the communications experiments requiring operation of the TWT. The maximum duration of any single pass for which the spacecraft is usable to the Andover, Maine, station is approximately 60 minutes.

The objective of 90 minutes per day for communications experiments may be distributed among the visible orbits with the possibility of equal distribution in three consecutive orbits.

2.1 *Solar Power Requirements*

The solar power plant requirements were calculated by considering the continuous and peak power requirements of the electrical systems, the efficiency of the regulator and converter, the battery efficiency, the eclipse time per orbit, the duty cycle of the various intermittent loads, the orbital period, and total light time per day.

The following formula was developed to determine the required power from the solar cell plant:

$$P_S = (W_S/T_L) = [(W_L + kW_D)/T_L] \tag{1}$$

where W_S = energy supplied by the solar source in one periodic interval,
W_L = energy consumed in the load during the light periods,
W_D = energy consumed in the load during the eclipse periods,
k = ratio of the energy put into the battery during charging to the energy available from the charged battery, and
T_L = light period.

The energy efficiency factor, k, is a complicated function which depends on battery temperature, charge rate, depth of discharge, discharge rate, charge time, and cycle behavior. Laboratory data on commercial nickel-cadmium storage cells evaluated during the early stages of Telstar system development indicated that a typical charging efficiency for sealed nickel-cadmium cells, based on deep discharges and charge rates of $C/50$* to $C/20$ for complete recharge, was approximately 55 per cent. The value of k for a charging efficiency of 55 per cent was calculated to be 2.23. This value of k was employed in determining the required solar cell power output. During the short development period there

* C is the current which would flow out of the battery during discharge if the nominal capacity of the battery could be removed in one hour at constant current.

were a number of revisions in the power requirements of the several electrical systems, and a considerable amount of necessary interaction among the various development activities. The maximum required solar power was calculated to be 14 watts using (1) and maximum load and eclipse requirements. Current data on the specially developed nickel-cadmium cell indicate that an energy ratio factor k of approximately 1.5 can be achieved in the required temperature range, with charge rates of $C/40$ to $C/10$.

Telstar employs 3600 n-p silicon solar cells, made up into 50 groups of cells in parallel, each group containing 72 cells in series. A silicon diode is placed in series with each parallel string to prevent cells which are not illuminated by the sun from loading the illuminated cells and also to prevent the battery from discharging into the solar cell plant. The solar cell arrangement occupies approximately 35 per cent of the exterior surface of the spacecraft.

2.2 *The Storage Battery*

The storage battery contains 19 specially prepared sealed nickel-cadmium cells with a nominal capacity of 6 ampere-hours. Fig. 3 is a photograph of the cell, which is discussed in detail in a companion paper.[1] The 19-cell battery is mounted in the canister in 3 groups of 5 cells each and 1 group of 4 cells. Each cell is individually insulated from the canister with a thin polyethelene sleeve.

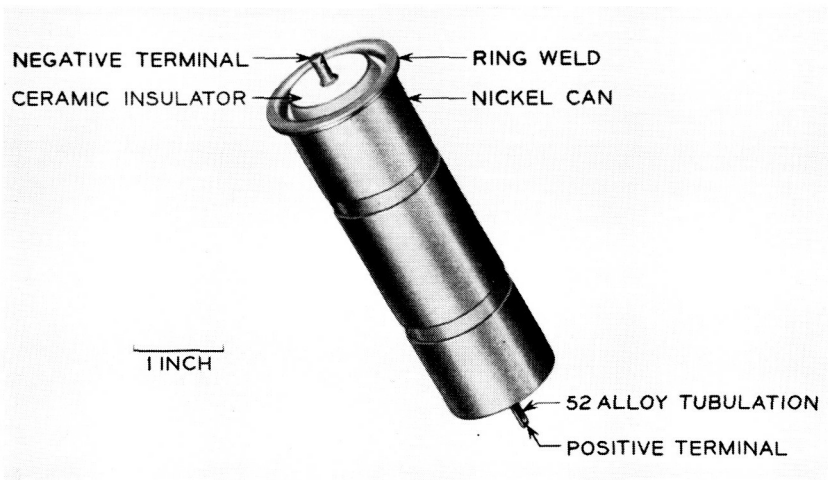

Fig. 3 — Nickel-cadmium cell for the spacecraft.

The battery is connected directly across the output of the solar cell plant through a diode normally bypassed by relay contacts. This diode circuit, called the "battery discharge gate," is described elsewhere in this paper. In this arrangement the maximum voltage of the solar power plant is 29.5 volts, which is the end-of-charge voltage of the 19-cell battery at the lowest expected temperature. The minimum voltage at the input to the main regulator is determined by the discharge voltage of the battery. The power system was designed to operate with a minimum voltage of 19.8 volts, based on 18 cells in the event of a short circuit of one cell.

2.3 *Main Regulator and dc-to-dc Converter*

The main regulator, shown in Fig. 2, provides a regulated voltage for the different loads from the varying battery voltage. A switching type series voltage regulator design was selected rather than quasi-linear series or shunt type regulators because of the higher efficiency that can be obtained with wide variations in battery voltage and load current. The main regulator provides three separate filtered outputs at nominally minus 16 volts. Separate filters are employed to reduce crosstalk between the command receivers, the radiation experiment and the switching transistor dc-to-dc converter. The efficiency of the regulator at maximum load is approximately 92 per cent.

The dc-to-dc high-voltage converter furnishes heater, anode, helix and collector voltages for the TWT, derived from the minus 16-volt supply. The converter is unregulated and its output regulation is governed by the changes in the minus 16-volt output of the main regulator and the load variations in the TWT. The over-all efficiency of the converter is approximately 70 per cent, including losses in the low-voltage command switching circuits. To conserve power, the converter is energized only during the communications experiment by sequential application of the TWT voltages by ground command.

The major items of the satellite power system are described in greater detail in the following sections, along with several auxiliary features.

III. NICKEL-CADMIUM STORAGE BATTERY

A sealed nickel-cadmium battery was selected for the spacecraft because this storage system is considered to be capable of

(a) accepting continuous overcharge during long periods of constant sunlight,

(b) displaying long cycle life under shallow depths of discharge and moderate life under deep discharges,

(c) being hermetically sealed, permitting long life in a space environment,

(d) operating in the temperature range of 15°F to 90°F, and

(e) providing nearly constant voltage during discharge.

3.1 *Battery Capacity*

Thermal calculations of the satellite chassis temperature indicated that the nominal battery temperature would be 70°F under conditions of initial available solar power of 14 watts and continuous sunlight. Data obtained with nickel-cadmium cells having a construction similar to those chosen for the power supply indicated that for a temperature of 70°F and a maximum cell voltage of 1.48 volts the overcharge current should not exceed $C/15$. Orbital predictions for the Telstar satellite indicated that early in life the satellite would be in continuous sunlight, under conditions of maximum available solar power, and would for long periods be operated with only the continuous power drain of the VHF beacon transmitter and command system. Under these conditions the charging power available to the battery would be approximately 10 watts, leading to a continuous charging current of approximately 0.36 ampere. To insure a safe continuous overcharge at this rate and a cell temperature of 70°F requires a cell having a nominal capacity of at least 5.4 ampere-hours. A smaller-capacity storage cell would require the addition of a battery charging current limiter.

In addition to the overcharge characteristics desired in the spacecraft battery because of long periods of continuous sunlight, consideration was necessarily given to the discharge capacity. Since the peak power required for a communications experiment exceeds the power available from the solar cells, the storage battery is subjected to many charge-discharge cycles during the satellite life. The battery is designed so that the peak load requirements can be met during at least three consecutive periods of longest eclipse. It is not feasible to completely recharge the battery during interim sunlight periods. Initially, 20 per cent was considered to be a safe maximum depth of discharge at the end of three peak eclipse time discharges. Each peak power drain represents a discharge of about 0.75 ampere-hour. Interim recharge is a function of the charge rate, cell temperature, and ampere-hour charge efficiency. For spacecraft nickel-cadmium cells the charge efficiency of partially discharged cells may range from 75 to 97 per cent. For the purpose of establishing a required cell capacity, the minimum recharge efficiency was used. Each charge interval between communications experiments returns approximately 0.5 ampere-hour; therefore at the end of the third consecu-

tive peak power drain, the capacity discharged from the battery is approximately 1.25 ampere-hours. Allowing this peak discharge to represent 20 per cent of the battery total capacity indicates that a 6.2-ampere-hour nominal capacity is required.

Consideration of the required continuous overcharge characteristics, along with the required discharge capacity, suggests that a battery having a nominal capacity of 6 ampere-hours is adequate for the spacecraft power system. Laboratory data on the power system performance obtained during the development program revealed satisfactory battery system behavior with maximum depths of discharge as high as 40 per cent when providing for frequent communication experiment usage during periods of greatest satellite visibility and maximum eclipse periods. Under these conditions, the battery may be discharged from a fully charged state during four consecutive orbits, with each discharge period equal to or greater than the maximum eclipse period. Fig. 4 illustrates the capacity removed from a fully charged storage battery as a result of the four consecutive peak power drains, three of which are

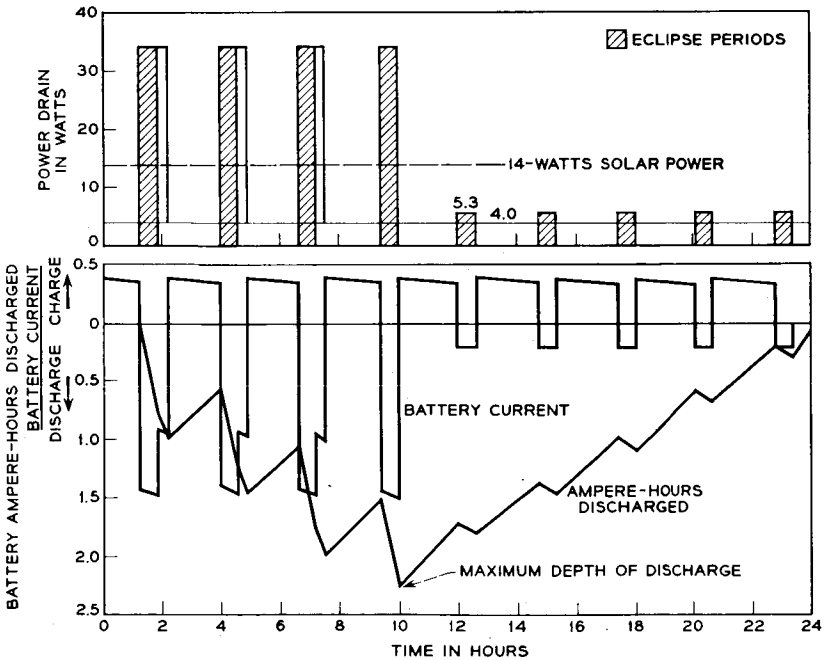

Fig. 4 — Battery charging and discharging, along with capacity removed from battery, during a typical 24-hour period.

for periods exceeding the maximum eclipse time. The maximum capacity removed is approximately 2.3 ampere-hours or 40 per cent of the available capacity of the battery, calculated on the basis of a charge efficiency of 75 per cent, a solar cell plant output of 14 watts, and illumination intervals and loads as shown in Fig. 4. This usage represents a large short-term discharge of the nickel-cadmium battery and requires that the sunlight periods during the balance of the day, approximately 11.5 hours in this illustration, be available for charging the battery to insure restoral of full battery capacity.

3.2 *Battery Energy Balance*

Analyzing the energy flow equations for the battery permits a flexible program involving communication experiments of varying duration. This analysis correlates the charging energy available from the solar cell plant, over any 24-hour period, with the energy requirements of the load. Thus, the power system designer can take into account different battery depths of discharge, reduced available solar cell power and different eclipse periods. Figs. 5 and 6 show the time allowable for com-

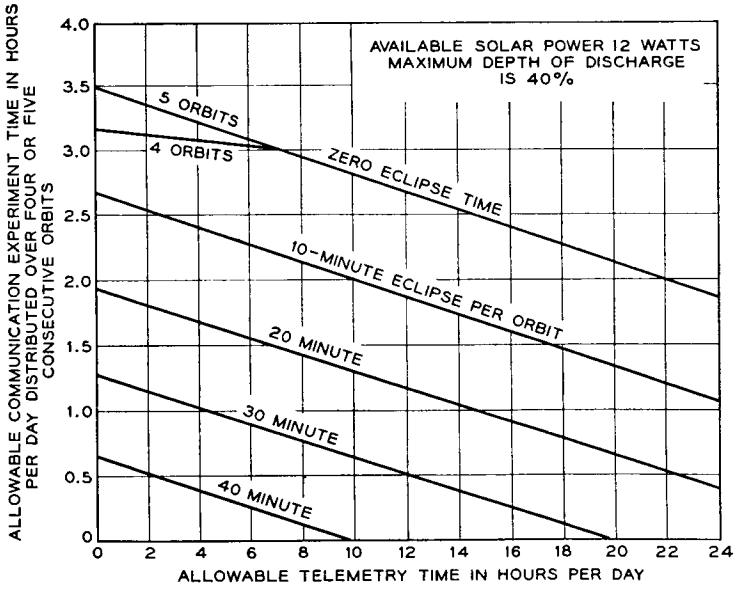

Fig. 5 — Allowable satellite utilization with communications experiments distributed over 4 or 5 consecutive orbits (solar power 12 watts).

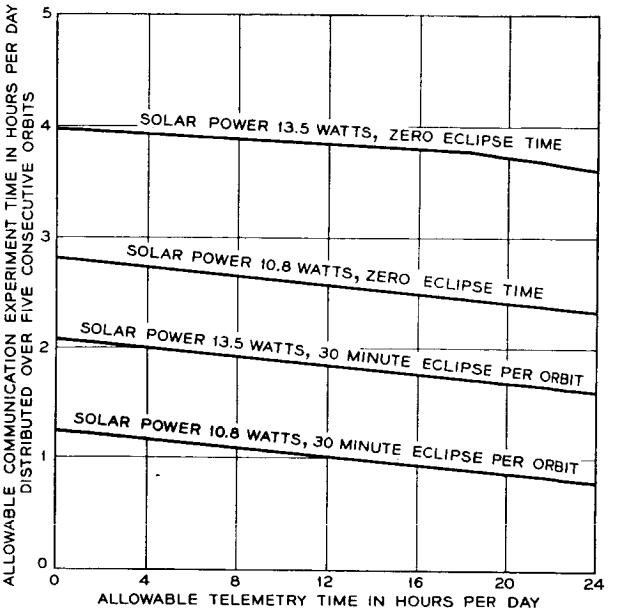

Fig. 6 — Allowable satellite utilization with communications experiments distributed over 5 consecutive orbits (variable solar power).

munication experiments as a function of the total time spent telemetering data to various ground stations. Families of such curves were developed for different values of available solar power, orbit eclipse time and battery depth of discharge, and for communication experiments distributed among 3, 4 and 5 consecutive orbits.

IV. MAIN REGULATOR

The principal function of the main regulator is to provide a regulated voltage with low ripple from the nickel-cadmium battery, whose voltage varies during the charge and discharge cycle. Fig. 7 is a photograph of the main regulator, packaged with a portion of the dc-to-dc converter. The main regulator is on the middle and bottom mounting boards of this package.

4.1 *Performance*

The main regulator supplies 16 volts ±0.17 per cent output, for loads varying between 0.2 and 2.0 amperes and an input voltage between 19.8

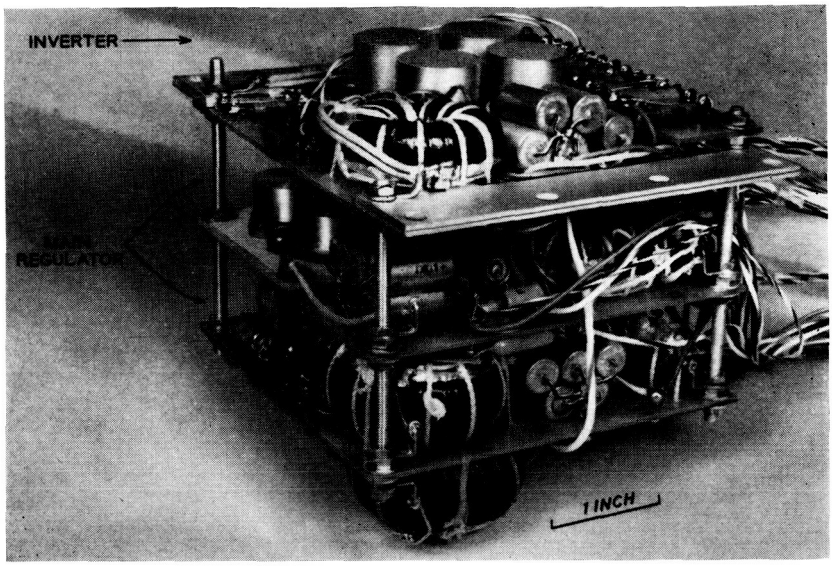

Fig. 7 — Main regulator assembly (unfoamed).

and 29.5 volts. The efficiency is approximately 92 per cent at maximum load and 85 per cent at minimum load.

Fig. 8 shows the basic performance characteristics of the regulator. Curves are drawn for conditions of minimum and maximum loading. The upper graph shows the output voltage vs input voltage; the flat portion is the region of regulation. The lower graph shows input current vs input voltage. The input current increases with input voltage until the minimum regulating voltage is reached. Then the input current falls off with increasing input voltage, since the regulator draws essentially constant power while regulating. Above the regulating range both the input current and output voltage increase with input voltage.

4.2 *Block Diagram of Main Regulator*

The block diagram of the main regulator is shown in Fig. 9. The dc input is "chopped" into a series of rectangular waves by means of a transistor switch. This switch is alternately a short circuit and an open circuit, dissipating relatively little power in either state.

The rectangular wave is imposed upon the main filter, a low-pass LC filter. The rectangular wave consists of alternate intervals of dc input voltage and ground; the main filter extracts the average of this

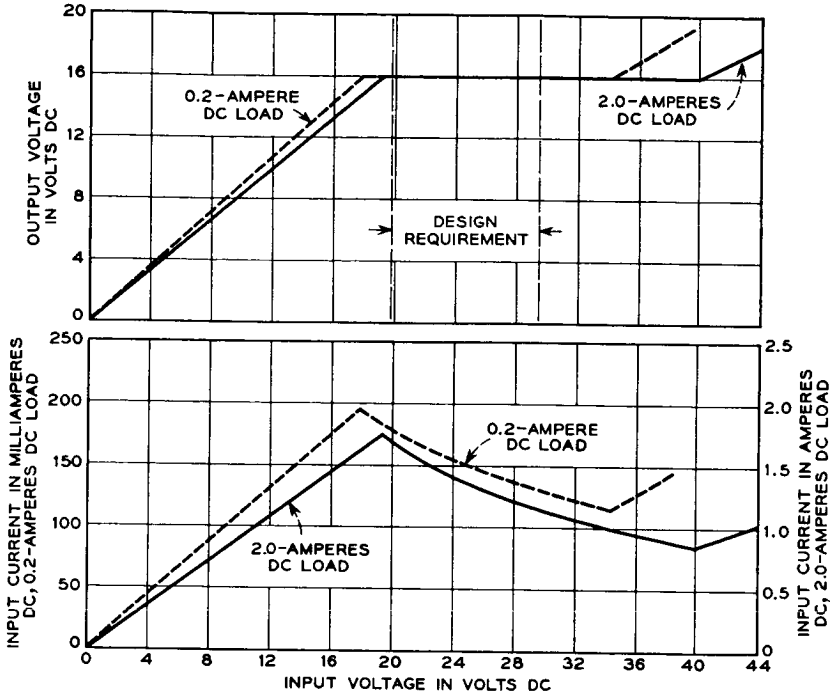

Fig. 8 — Main regulator nput-output characteristics.

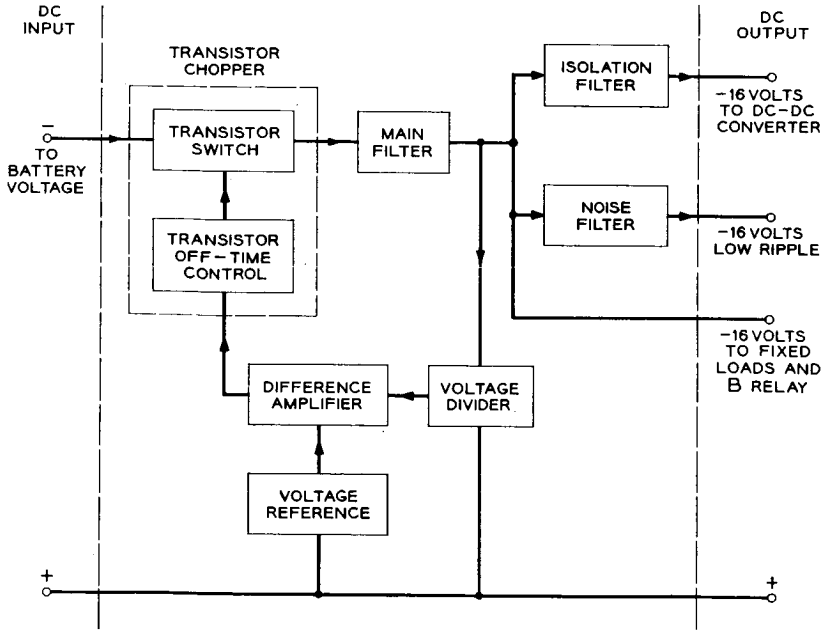

Fig. 9 — Block diagram of main regulator.

wave, which becomes the −16-volt output. Further filtering is provided by an isolation filter, which prevents interaction between the main regulator and the dc-to-dc converter. The noise filter provides an output whose fundamental component (at the main regulator frequency) is approximately 1 millivolt peak-to-peak.

The difference amplifier compares the output of the voltage divider, a fixed fraction of the output voltage (approximately 8.0 volts), with that of the voltage reference, a voltage regulator diode. If the output voltage goes above or below its correct value, an error signal is sent to transistor off-time control, which adjusts the off time, or time during which the transistor switch is an open circuit. This in turn controls the −16-volt dc output. The output voltage is thereby regulated by a closed feedback loop. The transistor switch and transistor off-time control can be considered as a single block, labeled "transistor chopper" in Fig. 9.

4.3 *Qualitative Discussion of Main Regulator*

4.3.1 *Design Approach*

Fig. 10 displays a simplified schematic of the transistor chopper. Transistor Q_1 is the switching power transistor, which alternates between cutoff and saturation to create rectangular waves. Since Q_1 regulates by

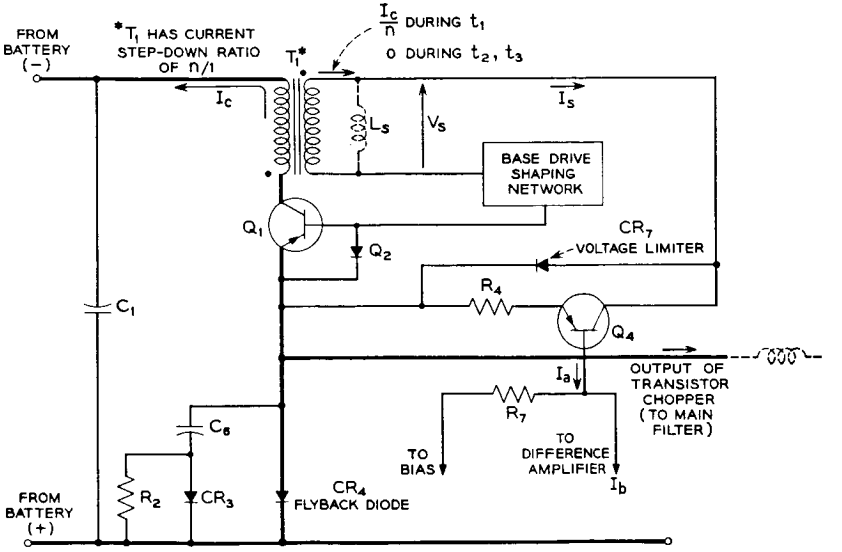

Fig. 10 — Simplified schematic main regulator of transistor chopper.

means of a switching mode, highly efficient regulation is possible. Given ideal components, a switching regulator can approach lossless regulation. This contrasts with the more familiar series or shunt type regulators where regulation is accomplished through a controlled dissipation of power.

While a switching regulator has the advantage of achieving high efficiency, it has the disadvantage of creating rectangular waves which must be filtered before application to the various loads. This filtering, to be efficient, is of the LC low-pass type and accounts for more than half the weight of the regulator. To minimize this weight it is desirable to switch at a relatively high frequency, where LC filtering is increasingly effective.

There are several practical limitations as to how high a frequency one can switch. First, there are the inevitable switching losses in transistor Q_1. While Q_1 dissipates little power in cutoff and saturation, the instantaneous power dissipated while switching from cutoff to saturation is high (roughly equal to one-half the input voltage multiplied by the load current, or 25 watts at 25 volts input and 2 amperes load), but the average loss is small because the switching times are very short compared to the over-all period. The power loss in Q_1 due to switching is approximately 0.5 watt. The switching frequency is approximately 20 kc at a 2-ampere load and 35 kc at a 0.2-ampere load.

The requirements for Q_1 were for a power transistor with fast rise and fall times and low saturation resistance (0.1 ohm). These requirements were met by an alloy-diffused germanium power transistor, a relatively recent semiconductor development. This type of transistor also proved to be less sensitive to proton bombardment than conventional germanium alloy power transistors.

The output of the transistor chopper feeds the inductor input filter (main filter). Diode CR_4, a flyback diode, maintains continuity of current in this inductor when Q_1 switches off. The network consisting of capacitor C_6, resistor R_2 and diode CR_3 improves the turn-off switching locus of transistor Q_1. Without this network, it would be necessary, on turn off, for Q_1 to block the entire input voltage, before CR_4 could start to conduct. However, with the network, C_6 charges up during the on time of Q_1 and can absorb current through C_6 and CR_3 as Q_1 starts to turn-off, without first requiring Q_1 to absorb the complete input voltage. Since C_6 charges and discharges every cycle, with power dissipated in R_2, it is obvious that losses in this network also increase with frequency.

Another source of frequency-dependent losses is the input inductor of the main filter. Here eddy current and hysteresis losses were minimized by the use of a powdered iron toroid.

Another frequency limitation besides losses is the storage time of transistor Q_1. While Q_1 has rise and fall times at least an order of magnitude shorter than those of a conventional germanium alloy transistor, its storage time is roughly equivalent (about 5 microseconds in a typical application). While the storage time does not appreciably affect efficiency, since Q_1 is saturated during this interval, it does affect frequency and the length of Q_1 on time, if it is allowed to become an appreciable percentage of the period. Since storage time is highly variable between transistors of the same code and also is reduced with time by proton radiation, it is desirable to have the circuit, rather than the storage time, predominate in controlling frequency.

Two other frequency limitations are the response times of transistor Q_4 and diode CR_4.

4.3.2 *Principle of Self-Excited Oscillations*

Transistor Q_1 in conjunction with current transformer T_1 forms a self-excited blocking oscillator. When Q_1 starts to turn on, the positive feedback polarity of T_1 causes current, I_s, to flow through CR_7 (forward biased), the emitter to base of Q_1 and the base drive shaping network, driving Q_1 further into saturation.

Inductor L_s represents the finite magnetizing inductance of the T_1 secondary. An ideal current transformer, of course, has infinite magnetizing inductance. The finite inductance of T_1 is deliberately controlled as a means of controlling the regulator switching frequency.

The waveforms of Fig. 11 relate the T_1 secondary voltage and current as a function of time and are idealized for simplicity. Assume Q_1 has just turned on. Then the current flowing out of the secondary of the "ideal" transformer is I_c/n, where I_c is the primary and transistor Q_1 collector current and n is the current stepdown turns ratio of T_1. Initially, L_s accepts no current and I_s, the "actual" transformer secondary current, is also I_c/n. This is displayed on the I_s waveform at $t = 0$. Since the idealized waveforms show a constant voltage, V_1, across T_1 secondary during the on time (t_1) of Q_1, then the current through L_s increases linearly with time, causing I_s to fall linearly with time. The total current out of the "ideal" secondary remains constant during t_1.

Since Q_1 has a large dc current gain (typically 150) over the load currents considered, it is reasonable to assume that I_s, which is also the base drive of Q_1, falls to zero before Q_1 switches off. At this time, the current through L_s is I_c/n, the entire "ideal" secondary current.

When Q_1 switches off, the "ideal" secondary current drops immediately from I_c/n to zero. At the same time, I_s reverses and initially becomes

$-I_c/n$ due to the demands of L_s. This current reverse biases Q_1 to maintain Q_1 in cutoff throughout the interval $t_2 + t_3$. Diode Q_2 bypasses the excess reverse current not needed to supply Q_1 reverse leakage currents.

Reverse current I_s passes through the parallel combination of CR_7 (reverse breakdown) direction and transistor Q_4. Resistor R_4 provides local negative feedback. At this point it is assumed that Q_4 acts as a current device, where collector current is independent of emitter-collector voltage. For a given value of I_s it is thus understood that either the base current to Q_4 is sufficient to saturate (zero voltage across Q_4) or the voltage across Q_4 is the breakdown voltage of limiter diode CR_7.

Referring once again to the waveforms of Fig. 11, t_2 is the interval during which limiter diode CR_7 conducts and t_3 is the interval during which Q_4 is saturated. The sum of t_2 and t_3 is the off time of Q_1. It will be noticed that T_1 secondary voltage, V_s, is much larger during t_2 (equal to $-V_2$) than during t_3 (equal to $-V_3$). As a consequence of this, I_s falls much more rapidly during t_2 than during t_3.

I_s is seen to fall rapidly till it reaches the value $-\beta I_a$, at which Q_4 saturates. β is the common-emitter current gain and I_a the base drive of transistor Q_4.

The off time of Q_1, and thus the dc output voltage, can be controlled

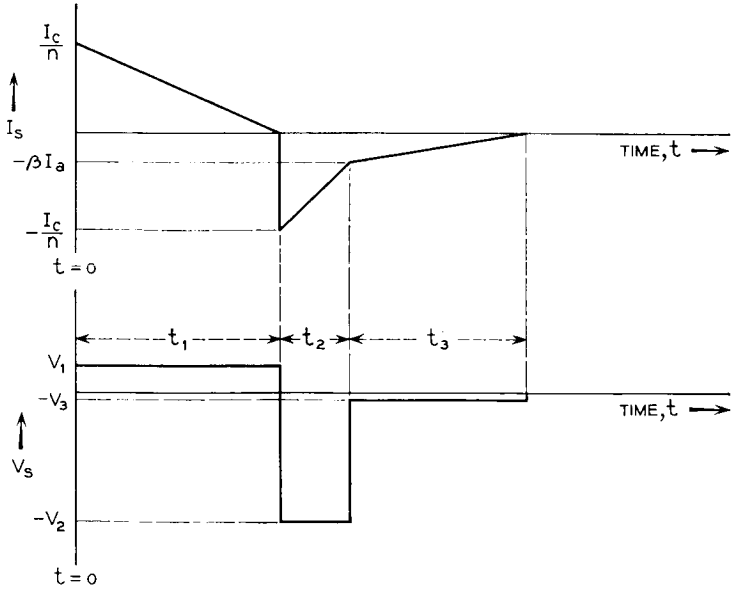

Fig. 11 — Waveforms of main regulator current transformer T_1.

by varying I_a . If I_a is zero, the reverse I_s will fall in the shortest possible time, minimizing the transistor Q_1 off time. If I_a equals $I_c/n\beta$, Q_4 will saturate as soon as Q_1 turns off, resulting in the longest possible off time. Regulation occurs only during the off time of Q_1 .

V. DC-TO-DC CONVERTER

The dc-to-dc converter furnishes high and low dc voltages for the TWT and a low dc voltage for the bias for the down converter. Important in the derivation of these voltages is the dc-to-ac inverter shown on Fig. 12; this inverter changes the −16-volt dc input voltage to an ac voltage which is applied to transformers. The secondaries of the transformers are applied to rectifiers and filters to obtain dc voltages. The converter is unregulated, and its output regulation is the sum of changes due to temperature and to load variations in the TWT. The over-all converter efficiency is approximately 71 per cent. A simplified diagram of the dc-to-dc converter is shown in Fig. 13.

To conserve power, the converter is energized only during the communications experiment. Command signals to the satellite to operate the traveling-wave tube and bias the down converter of the transmission equipment are accomplished by use of three magnetic-latching relays mounted in the power supply.[3] Relay A responds to the A command to the satellite, which causes the heater voltage to the TWT and the positive bias voltage for the down converter to be applied.[4] The B relay responds to the B command and causes the helix and collector voltages to be applied but no beam current to flow in the TWT when B relay is

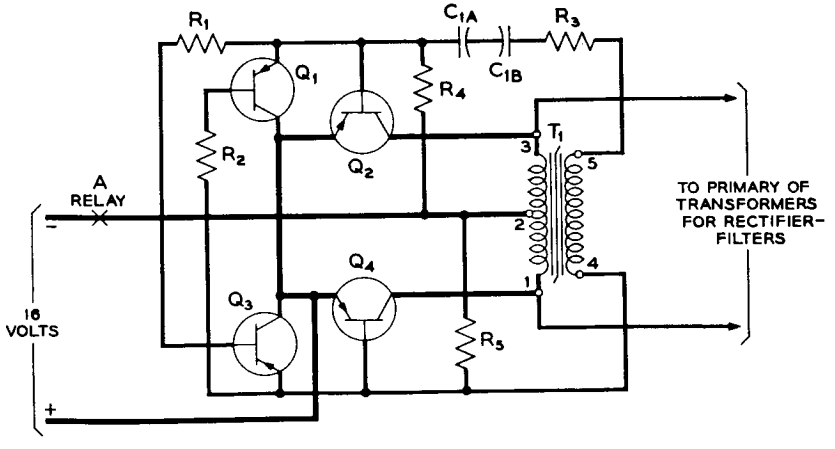

Fig. 12 — Schematic diagram of dc-to-ac inverter.

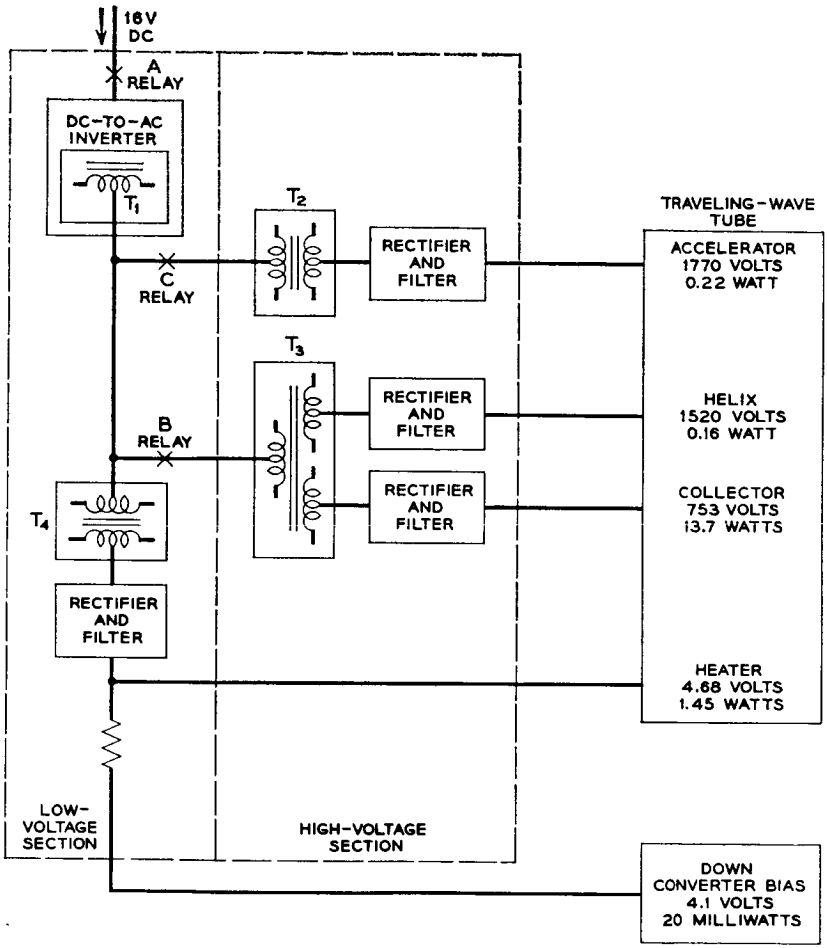

Fig. 13 — Block diagram of dc-to-dc converter.

closed. Beam current flows when the A, B and C relays are commanded on. This eliminates the possibility of other voltages being applied to the TWT prior to the heater voltage. After a minimum of three minutes warm-up time for the heater of the TWT, the C command to the satellite causes the accelerator voltage to be applied to the TWT. The CC command causes the accelerator voltage to be removed. The A and B relays respond to the AA command on turn-off. Switching in the low-voltage ac circuits provides a satisfactory means of effectively switching the high voltage to the TWT through the use of separate transformers for the helix-collector and accelerator rectifiers. The primaries of the transform-

ers are connected as required by the B and C relays to the dc-to-ac inverter. The inverter is operated from the −16-volt dc source by the A relay being commanded on.

5.1 *DC-to-AC Inverter*

A schematic diagram of the inverter is shown in Fig. 12. The inverter produces a square-wave ac voltage with a nominal frequency of 2.5 kc at full load. This frequency is selected to provide minimum transistor switching and transformer losses. Also, it is desirable that the switching frequency of the dc-to-ac inverter be separated from the switching frequency range of the −16-volt regulator. The dc-to-ac inverter, along with relays D, E and F, is mounted in the main regulator package. The D relay causes −16 volts to be applied to the converter for the TWT heater telemetry network in addition to applying −16 volts to other circuits in the satellite. Relay E is used to apply voltage to the orientation loop and relay F is used to switch operation of encoders 1 or 2.

A feedback winding on transformer T_1 (shown in Fig. 12) is provided to furnish the source voltage for the drive circuit of the "on" power transistor, Q_2 or Q_4. The simplified drive circuit shown in the schematic of Fig. 14 may be used to describe operation during the half-cycle that transistors Q_3 and Q_2 are conducting and transistors Q_1 and Q_4 are cut off.

The inverter-transformer saturates each half-cycle and transformer action ceases, so that the feedback voltage on the secondary winding collapses. This causes the "on" power transistor to fall out of saturation because of lack of base drive current necessary to maintain low emitter-to-collector voltage. Consequently, the voltage applied to the primary

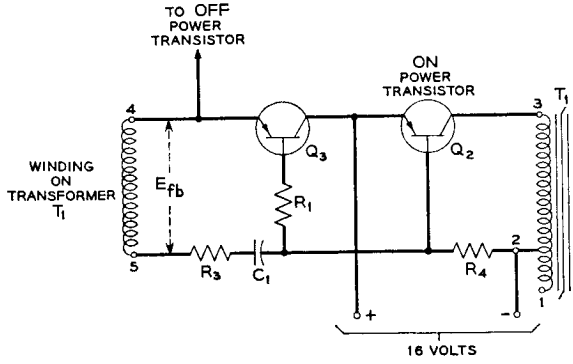

Fig. 14 — Simplified schematic of inverter drive circuit.

winding of transformer T_1 is reduced, causing a further reduction of feedback voltage. This action results in turning off the conducting transistor and turning on the transistor that has been cut off.

Since the power transistors require a finite time to turn off because of the storage time of the transistor, it is necessary to provide switching of the transistors so that at no time are transistors Q_2 or Q_4 conducting simultaneously. The collector current of the conducting transistor, Q_2 or Q_4, increases when transformer T_1 saturates because of the effective low impedance in the collector circuit. This increased current causes an increase of the power dissipation during switching of each half-cycle. To limit these losses and improve reliability, the base current of the power transistors is just sufficient to cause saturation at the time prior to turn-off but not large enough to cause excessive storage time. This is a value of base current determined for an expected degradation of gain due to aging and radiation damage. The base current is made large enough at the turn-on portion of the cycle to provide fast switching at each half-cycle, and the feedback is sufficient to initiate and maintain oscillation when the A, B, or C relays operate. The power transistor losses can be divided into three classifications: conduction, switching, and cutoff. The conduction losses are minimized by operating the power transistors in a saturated mode. The loss during switching is reduced by limiting the rise of collector current when the inverter-transformer saturates at the end of each conduction cycle. The drive circuit also provides negative base current to sweep out the minority carriers of the conducting transistor and reduce the transistor storage time. This helps prevent both power transistors from being on simultaneously, a condition which could result in catastrophic failure. Resistor R_4 provides initial base current to power transistor Q_2 when the A relay is commanded on. The magnitude of the base current is large enough to insure reliable starting of the inverter.

The base current for transister Q_2 (shown in Fig. 14) prior to switching is

$$i_{fb} = \frac{E_{fb} + (q_0/C_1)}{R_T} \exp - \frac{t_1}{R_T C_1}$$

where

E_{fb} = voltage of secondary winding on T_1

q_0 = charge on C_1 at time of switching

$t_1 = 1/2f$, where f is the switching frequency, and

R_T = effective resistance of driver circuit for "on" transistor Q_2.

Also

$$R_T \approx R_3 + \frac{R_1}{h_{FE} \text{ of } Q_3}.$$

The waveform of the drive current is shown in Fig. 15.

When the A command is sent to the satellite, the −16 volts is applied to the inverter input. Oscillation is initiated and the output of the rectifier-filter provides power for the heater of the TWT. At the instant

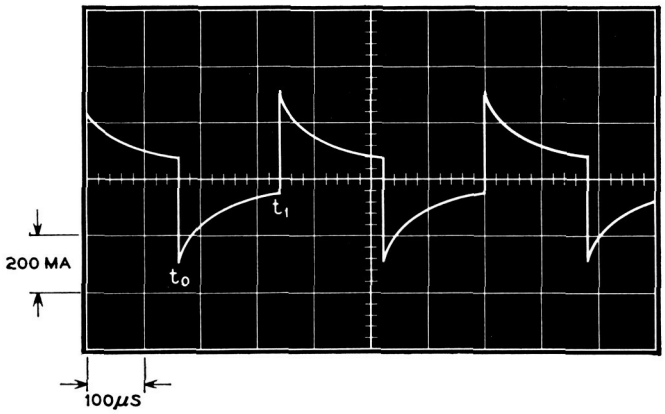

Fig. 15 — Waveform of inverter feedback current.

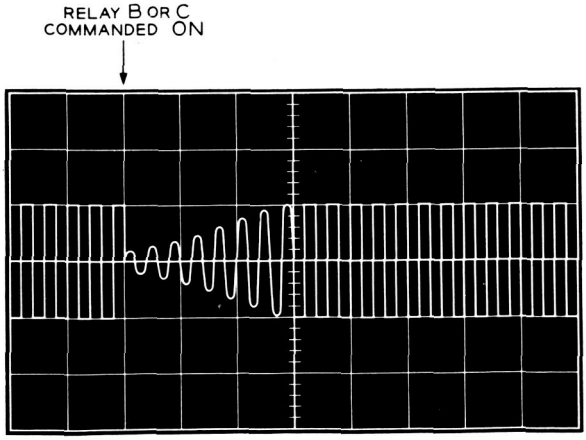

Fig. 16 — Inverter output voltage when relays B or C are commanded on.

the B and C relays operate, an effective short is placed on the output of the inverter due to the inrush current of the transformers connected when each relay operates. Also, the high-voltage capacitors in the rectifier-filter tend to draw large initial surge currents. To prevent excessive transistor collector power dissipation due to these transients, the drive circuit is designed to cause a gradual buildup to steady-state operation. Fig. 16 indicates the waveform produced on the output of the inverter when relay B or C is commanded on.

5.2 *Rectifier-Filter*

A photograph of the rectifier-filter section of the TWT power supply is shown in Fig. 17. Included in this unit are the telemetry networks for the heater voltage, collector, helix and accelerator currents.

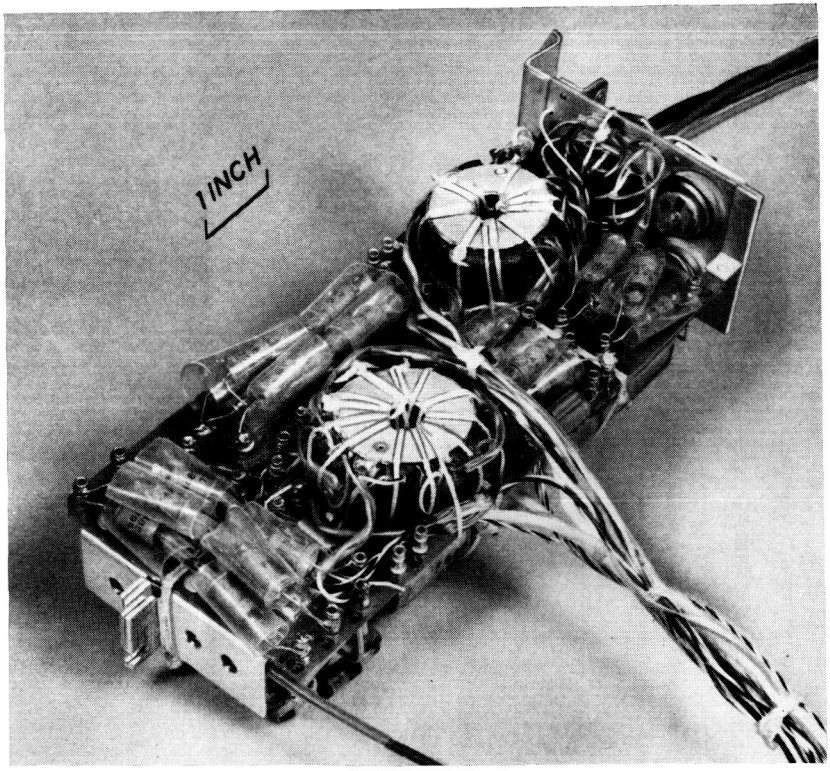

Fig. 17 — Traveling-wave tube power supply.

5.2.1 *Heater*

The square-wave ac voltage across the full primary of the inverter-transformer T_1 of Fig. 12 is applied to the primary of the heater-transformer, T_4, which provides bias and collector voltages for the transistorized synchronous rectifier Q_1 and Q_2 as shown in Fig. 18. The low voltage drop between the emitter and collector of the conducting transistor and

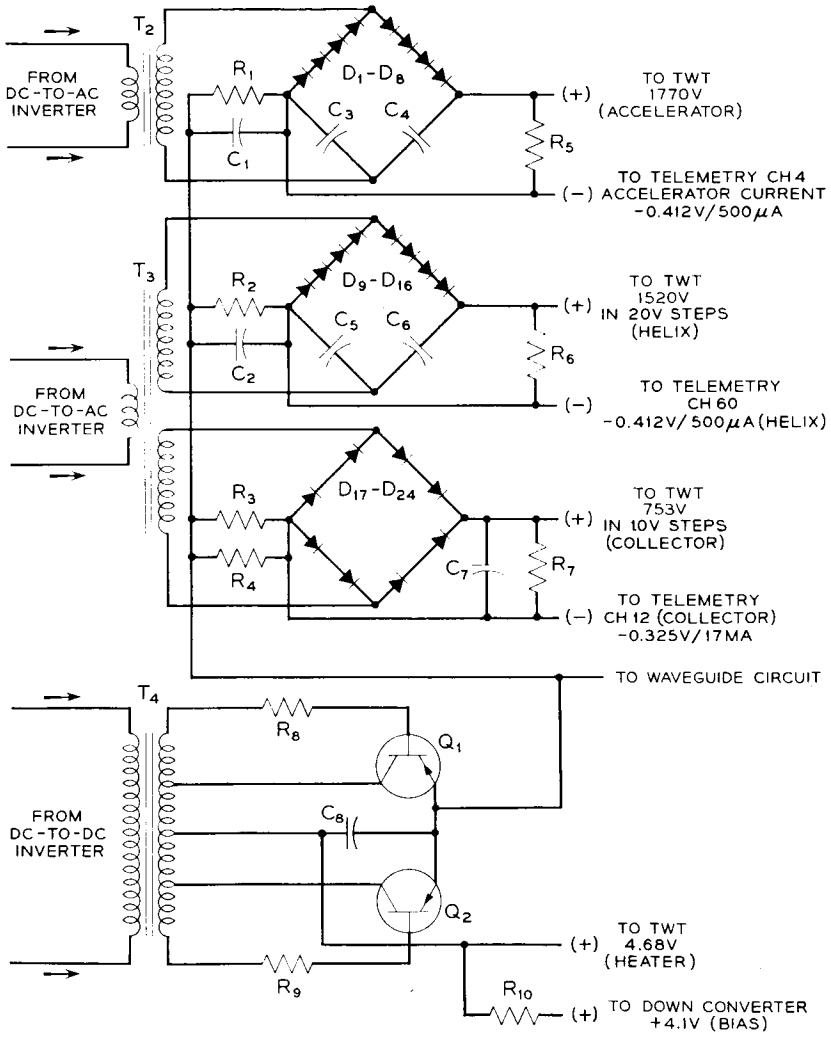

Fig. 18 — Schematic of traveling-wave tube power supply.

the small power necessary to maintain saturation affords an efficient means of obtaining dc for the heater of the TWT. Since the output is a rectified square-wave voltage, sufficient filtering is accomplished with only a capacitor filter.

5.2.2 *Helix-Collector*

Two separate secondary windings on transformer T_3 (shown in Fig. 18) provide helix and collector voltages for the TWT. One secondary winding is connected to a full-wave bridge rectifier and capacitor filter to obtain the dc voltage for the collector, and the other is connected to a voltage doubler rectifier-filter to obtain the dc voltage for the helix. A bleeder resistance across the collector output is provided to discharge the capacitor. Also, the bleeder in the helix rectifier prevents a rise of voltage at very low helix currents of 20 to 40 microamperes.

5.2.3 *Accelerator*

A separate transformer with one secondary is used to furnish high voltage for the voltage doubler rectifier-filter to obtain the dc voltage for the accelerator of the TWT. It is necessary to use a bleeder resistor to discharge the capacitors of the voltage doubler to prevent damage to the TWT.

5.3 *Performance*

5.3.1 *Heater* (A *Command On*)

Since the TWT heater resistance, when cold, is estimated to be approximately one-sixth the hot or steady-state resistance, there is a tendency for the heater to draw large initial current. Operational tests indicate that several cycles of the dc-to-ac inverter are required for the heater voltage to build up to full output. Steady-state operating temperature of the TWT heater is reached in approximately three minutes. The heater voltage is approximately 4.5 per cent higher with only the heater on than when the A, B, and C relays are on. This is due to the light load on the converter until there is TWT beam current. The slight over-voltage helps the TWT tube heater to stabilize in the three-minute warmup period.

5.3.2 *Heater, Collector and Helix* (A *and* B *Commands On*)

Since no beam current exists until the accelerator voltage is applied, there is a tendency for high voltage to be produced on the collector and

helix outputs during the time before the accelerator voltage is applied to the tube. A fixed minimum resistance load in the power supply reduces the rise of voltage on the collector of the TWT to less than 1150 volts, which is the maximum safe voltage for the filter-capacitor, transformer and TWT.

5.3.3 *Heater, Collector, Helix and Accelerator* (A, B, *and* C *Commands On*)

With the C relay on, there exists collector current of approximately 18 milliamperes, helix current between 20 and 50 microamperes with no RF drive to the TWT and 100 to 300 microamperes with RF drive, and an accelerator current between 100 and 150 microamperes. This current may build up to 500 microamperes after a year of operation in space. The most critical voltage on the TWT is the helix voltage. The regulation of this voltage is improved by designing the collector-helix transformer to have minimum leakage reactance on the helix winding of the transformer.

The power supply and TWT of each satellite are tested together prior to installation in the canister of the satellite. The final voltage and currents for optimum performance of the TWT are determined by observing the variation of RF output of the TWT when different voltage taps are selected on the transformers of the converter. The 16-volt dc input to the inverter is varied ±3 per cent, and taps are selected which give the smallest variation of RF output with the change of voltage to the TWT.

Measurements on the power supply and TWT of the spacecraft are given in Table I.

The total output power of the converter when the TWT is on is 15.48 watts. The input power is 21.8 watts. The efficiency is 71 per cent. The input current to the dc-to-ac inverter is 1.36 amperes. The bias voltage

TABLE I—MEASUREMENTS OF POWER SUPPLY AND TWT OF SPACECRAFT

Command	Item Measured	Volts	Current	Ripple
A only	heater	4.89	322 ma	
A + B	heater	4.850	320 ma	
	collector	1035	0	
	helix	1710	0	
A + B + C	heater	4.68	310 ma	135 mv
	collector	753	18.1 ma	310 mv
	helix	1520	110 μa	800 mv
	accelerator	1770	125 μa	600 mv
	down-converter bias	4.1	4.8 ma	

for the down converter is derived from the same rectifier-filter used to supply the heater voltage.

5.4 *Operational Tests*

The dc-to-ac inverter is combined with the −16-volt regulator to form a subassembly, and tests are made with the rectifier-filter section of the converter. The two units are foamed and then temperature cycled. The two subassemblies are soaked at −22°F and +140°F for six hours at each temperature. An operational temperature run is performed between +15°F and +105°F.

The −16 volts is operated continuously during the vibration test, and the states of relays A, B, C, and D are monitored. A change of state of the relays would have indicated that the TWT could have come on during launch.

Temperature cycling of the power supply in the canister includes soaking at 0°F and +125°F, and operation between +25°F and +90°F. During shake and environmental tests at Whippany[5] and extended transmission tests at the Murray Hill Laboratories, data from the power supply telemetry channels are evaluated to confirm that the power supply is performing satisfactorily.

VI. CONSTRUCTION FEATURES

Design and construction changes during the development period included the placement of aluminum caps on the transistors of the main regulator and inverter to reduce the effect of radiation damage. Separation of the high and low potential terminal posts gave greater assurance that corona would not occur.

VII. AUXILIARY FEATURES

7.1 *Two-Year Timer*

It was required that two years after spacecraft launching the VHF beacon of the satellite be irrevocably turned off to clear the radio channel; this is to be done by a timer which operates from an independent source of power. The timer consists of a tuning fork mechanically coupled to a gear train and switch to disconnect power to the VHF beacon transmitter. The oscillation of the tuning fork is maintained by means of a 360-cycle transistor oscillator driven by a battery. The power source is a single primary mercury cell with sufficient ampere-hour capacity to supply the current for 18,000 hours.

7.2 *Battery Discharge Gate*

There was need for a means to control remotely the discharge of the Ni-Cd battery by removing the loads after sealing the canister prior to launching. This switch must not prevent the charging of the battery by the solar cell plant. To perform this switching function a silicon diode, used as a gate, was connected in series with the battery. The diode was connected, as shown in Fig. 2, with its polarity in a direction to allow the solar cell plant to charge the battery, with the loss of its forward drop of approximately one volt. When load is to be supplied from the battery, the contacts of the S relay short out the diode. The S relay is operated under control of the command receiver in the satellite or by means of the low-voltage cutoff circuit.[3]

Before launching, the S relay is open and the diode gate prevents discharge of the battery between tests and during shipment. After launching, if it is determined from telemetered data that the battery is excessively discharged due to long periods of transmission, or due to low solar cell output voltage which could occur during extended periods of polar illumination of the satellite, the S relay can be opened to disconnect the load from the battery. The command receiver will operate with power from the solar cell plant, through the main regulator, making it possible to command the S relay to close, shorting the diode gate.

7.3 *Pre-Launch Test and Auxiliary Power Supply*

During the testing period of the satellite on the ground and during the launching period, the solar cells are not illuminated, so that an auxiliary source of power is required. A passive ferroresonant regulating circuit was used to eliminate the effects of input ac line voltage variations and limit the charging current to the maximum safe value for the nickel-cadmium battery.

VIII. PERFORMANCE

The performance of the Telstar power system has agreed very closely with the design objectives. Voltage requirements of all active elements of the satellite have been met, as evidenced both by the results of measurements before launch and by telemetry data after launch. The main regulator has successfully adjusted for a wide range of input voltage, as shown in Fig. 19. This figure presents the battery voltage time history for three different satellite passes within range of the Andover ground station.

The voltage behavior for orbit 414 is typical of an orbit in full sun-

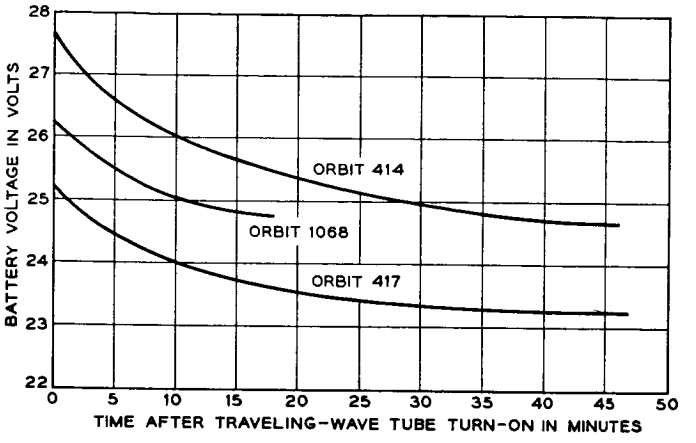

Fig. 19 — Input voltage to main regulator.

light with the battery fully charged at the beginning of the orbit; the communications experiment was in operation for nearly 50 minutes. A similar communications experiment was performed during orbits 415, 416 and 417. The voltage record for orbit 417, shown in Fig. 19, shows a substantially lower initial value as a result of battery discharge; at the end of orbit 417 the battery had been discharged to 60 per cent of its capacity.

The voltage data for orbit 1068 show a low initial voltage despite the fact that the battery was fully charged initially, for the reason that the satellite was in eclipse for the first 10 minutes of the orbit.

The state of charge of the battery has been monitored carefully through detailed histories of charge and discharge currents. These histories take into account actual solar plant current and actual load currents as reflected in telemetry data. Satellite use has been programmed so that at no time has the battery been discharged below 60 per cent of capacity.

IX. ACKNOWLEDGMENTS

Acknowledgment is hereby made of the contributions of many members of the Power Systems Laboratory, too numerous to mention by name.

REFERENCES

1. Bomberger, D. C., and Moose, L. F., Nickel-Cadmium Cells for the Spacecraft Battery, B.S.T.J., this issue, Part 3.

2. Feldman, D., and Thomas, U. B., Current Status of Sealed Nickel-Cadmium Storage Cells, Proc. of 1962 A.I.E.E. Pacific Energy Conversion Conference.
3. Chapman, R. C., Jr., Critchlow, G. F., and Mann, H., Command and Telemetry Systems, B.S.T.J., this issue, p. 1027.
4. Davis, C. G., Hutchison, P. T., Witt, F. J., and Maunsell, H. I., The Spacecraft Communications Repeater, B.S.T.J., this issue, p. 831.
5. Delchamps, T. B., Jonasson, G. C., and Swift, R. A., The Spacecraft Test and Evaluation Program, B.S.T.J., this issue, p. 1007.